

INVARIANTS OF VELOCITY GRADIENT TENSOR IN COMPRESSIBLE PIPE, NOZZLE AND DIFFUSER FLOWS

Komal Kumari, Somnath Ghosh

Department of Aerospace Engineering,
Indian Institute of Technology, Kharagpur, India
sghosh@aero.iitkgp.ernet.in

Joseph Mathew

Department of Aerospace Engineering,
Indian Institute of Science, Bangalore, India

ABSTRACT

Velocity gradient tensor (VGT) analysis of high-order accurate DNS data of compressible pipe, nozzle and diffuser flows is performed. Joint pdfs of second and third invariants conditioned on positive and negative dilatation levels are presented in the viscous layer, buffer layer, log layer and core regions of these flows. For flow regions with positive dilatation there is a preference for unstable flow topology, while regions with negative dilatation show a preference for stable flow topology.

INTRODUCTION

Analysis of velocity gradient tensor (VGT) in turbulent flows (Chong *et al.*, 1990) to study the local flow topology has been the focus of many studies in literature with the aim of gaining a better understanding of the dynamics of small scales. VGT analysis of incompressible channel flow was carried out by Blackburn *et al.* (1996) using DNS data where the typical teardrop shape (i.e. a preference for 2nd and 4th quadrants) of the joint pdf of Q and R (2nd and 3rd invariants) was noticed in the buffer layer, log layer and the outer layer. This behaviour has also been observed in incompressible mixing layers (Soria *et al.*, 1994). DaSilva & Pereira (2008) analysed VGT invariants near the turbulent-nonturbulent interface of incompressible mixing layers using DNS and showed that the characteristic teardrop shape of $Q - R$ is not yet formed at the interface but at a distance of the order of Kolmogorov scale away from the interface. Compared to incompressible flows, studies of topology of small scale motions based on VGT for compressible flows have been fewer. Pirozzoli & Grasso (2004) confirmed the teardrop shape for 2nd and 3rd invariants of the anisotropic part of the VGT for compressible isotropic turbulence. Suman & Girimaji (2010) looked at the joint pdf of Q and R for different levels of dilatation and found that the teardrop shape appears only when the dilatation is zero but the shape changes for positive and negative dilatation indicating different local flow topologies due to compressibility effects. Wang & Lu (2012) performed VGT invariant analysis of a supersonic boundary layer and observed that the flow topology changes when dilatation is significant. A recent analysis of DNS data of temporal compress-

ible mixing layers by Mathew *et al.* (2016) showed a new topology at the turbulent/nonturbulent interface when the convective Mach number was high. It was shown that at high Mach numbers the entrainment can also be through tube-like structures alongwith the dominant mechanism of entrainment through sheets. To the best of our knowledge VGT invariant analysis based on DNS data of supersonic channel and pipe flows have not been carried out till now. In this study we perform VGT invariant analysis for supersonic pipe, nozzle, diffuser flows using high-order accurate DNS datasets. The aim is to observe the effects of dilatation (both positive and negative) on the local flow topology in these canonical supersonic wall-bounded flows.

MATHEMATICAL AND COMPUTATIONAL DETAILS

Following Chong *et al.* (1990), the local flow topology at a given point in the flow can be assessed with the knowledge of the eigenvalues (λ) of the velocity gradient tensor A_{ij} . The characteristic equation satisfied by these eigenvalues is

$$\lambda^3 + P\lambda^2 + Q\lambda + R = 0 \quad (1)$$

where the invariants P, Q, R have the following form:

$$P = -tr[A_{ij}] = -S_{ii}; Q = 0.5(P^2 - tr[A_{ij}^2]); R = -det[A_{ij}]$$

Hence P is zero for incompressible flows but will be nonzero (both positive and negative) when the flow is compressible. As explained in Chong *et al.* (1990) and Suman & Girimaji (2010), the $Q - R$ plane is partitioned (by dashed lines in the bottom half of the figures presented here) into regions of real and complex roots of eq. 1. The region of complex roots is further divided by a line which contains points having purely imaginary roots. The DNS datasets analysed here have been presented in Ghosh & Friedrich (2014). The governing equations for compressible flow written in generalized curvilinear coordinates in a characteristic form (Sesterhenn, 2001) involving the primitive variables

pressure, velocity and entropy are solved using the 5th order compact upwind finite difference scheme of Adams & Shariff (1996) to discretise the convection terms while the 6th order compact central scheme of Lele (1992) is used for the molecular transport terms. Time integration is carried out using a low-storage 3rd order Runge-Kutta scheme (Williamson, 1980). The velocity gradient tensor used for the analysis is also computed with the 6th order compact central scheme. The supersonic turbulent pipe flow which also acts as inflow condition for the diffuser flow has a centerline Mach number (M_c) of 1.8 and friction Reynolds number (Re_τ) of 300. The inflow for the nozzle is also from a different turbulent compressible pipe flow simulation at $M_c = 1.5$ and $Re_\tau = 245$. The pipe flow simulations use streamwise periodic boundary conditions and isothermal wall and are coupled to the nozzle/diffuser flow simulations at every time step using MPI routines. The diffuser (nozzle) simulations use isothermal wall and partially nonreflecting outflow conditions. Resolution used for the pipe flow in axial, azimuthal and radial directions is $256 \times 256 \times 140$; for the nozzle flow it is $256 \times 128 \times 91$ and for the diffuser it is $384 \times 256 \times 140$.

RESULTS

The flows analysed here have been extensively studied in Ghosh & Friedrich (2014). In the supersonic pipe flow with isothermal wall, the near-wall variation in density results in a change in Reynolds stress anisotropy when compared to the incompressible pipe. This occurs due to reduction in pressure-strain correlations at high Mach number. Change in density in streamwise direction due to flow expansion or compression in the supersonic nozzle or diffuser is one of the reasons for substantial decrease/increase in turbulence intensities in these flows. Reduction/increase of pressure-strain correlation also leads to a decrease/increase of turbulence intensities in these flows (see Ghosh & Friedrich (2014) and references therein). In this study, we analyse instantaneous snapshots of the three dimensional velocity fields. We first look at the pdf of dilatation (i.e. the negative of it) in pipe, nozzle and diffuser flows in fig. 1. We note that in the pipe flow the pdf profiles for the different layers are centered around $P = 0$. In the nozzle flow, the pdf profiles are skewed towards positive dilatation, as expected. As we move from the viscous layer to the core region, the pdf profiles move progressively towards the positive dilatation side. In the diffuser flow, the profiles are skewed towards negative dilatation. Here also we observe a progressive shift of the profiles towards the negative dilatation side as we move from viscous layer to the log layer. However, the core region profile shifts by a lesser extent than the buffer layer profile in this case. We now present joint pdfs of Q and R (normalized using the centerline velocity and radius of the pipe), conditioned on specific dilatation levels in the viscous sublayer, buffer layer, log layer and core region of the pipe, nozzle and diffuser flows in figures 2 to 4. The pdfs are calculated using flowfields at a particular time instant by taking all points for a particular layer for the pipe flow and taking points lying in the first half of the nozzle at a given layer. The 3σ range was divided into 200 equispaced bins for calculating the pdfs. As seen in the pipe flow (fig. 2), when dilatation is positive, unstable topologies are preferred i.e. a majority of the points lie in the 2nd and 4th quadrants. This implies that expansion regions are dominated by vortex stretching and sheet-

like structures. On the other hand, when dilatation is negative, majority of the points are concentrated in the 1st and 3rd quadrants which means that stable topologies are preferred. Hence, regions of compression are associated with vortex compression and tube-like structures. These trends are found in all the layers and are in qualitative agreement with those found in compressible isotropic turbulence by Suman & Girimaji (2010). In the nozzle flow (fig. 3), we observe a preference for unstable topologies (vortex stretching and sheet-like structures) in regions of expansion especially in the log layer and the core region, where a strong preference for sheet-like topology can be seen. A similar (albeit weak) tendency is observed in the buffer layer, while the viscous sublayer does not exhibit such a trend, in contrast to the findings for pipe flow. In the diffuser flow (fig. 4), we see a preference for stable topologies in the viscous layer, log layer and core region but not in the buffer layer.

CONCLUSIONS

Velocity gradient tensors of supersonic pipe, nozzle and diffuser flows are analysed using high-order accurate DNS data. In the pipe flow, regions of positive and negative instantaneous dilatation appears with nearly equal probability. In the nozzle flow there is a dominance of positive dilatation while in the diffuser flow negative dilatation dominates. Joint pdfs of Q and R conditioned on positive and negative dilatation reveals the effect of dilatation on the local turbulence structure. Regions with positive dilatation are mostly associated with vortex stretching and sheet-like structures (unstable topology) while those with negative dilatation show preference for vortex compression and tube-like structure (stable flow topology).

REFERENCES

- Adams, N. A. & Shariff, K. 1996 A high-resolution hybrid compact-ENO scheme for shock-turbulence interaction problems. *Journal of Computational Physics* **127**, 27–51.
- Blackburn, H.M., Mansour, N.N. & Cantwell, B.J. 1996 Topology of fine scale motions in turbulent channel flow. *Journal of Fluid Mechanics* **310**, 269–292.
- Chong, M.S., Perry, A.E. & Cantwell, B.J. 1990 A general classification of three-dimensional flow fields. *Phys. of Fluids A* **2**, 765–777.
- DaSilva, C.B. & Pereira, J.C.F. 2008 Invariants of the velocity-gradient, rate-of-strain, and rate-of-rotation tensors across the turbulent/non-turbulent interface in jets. *Physics of Fluids* **20**, 055101–1–055101–18.
- Ghosh, Somnath & Friedrich, Rainer 2014 Effects of distributed pressure gradients on the pressure-strain correlations in a supersonic nozzle and diffuser. *Journal of Fluid Mechanics* **742**, 466–494.
- Lele, S.K. 1992 Compact finite difference schemes with spectral-like resolution. *Journal of Computational Physics* **103**, 16–42.
- Mathew, J., Ghosh, S. & Friedrich, R. 2016 Changes to invariants of velocity gradient tensor at the turbulent-nonturbulent interface of compressible mixing layers. *International J. of Heat and Fluid Flow* **59**, 125–130.
- Pirozzoli, S. & Grasso, F. 2004 Direct numerical simulations of isotropic compressible turbulence: influence of compressibility on dynamics and structures. *Physics of Fluids* **16**, 4386–4407.
- Sesterhenn, J. 2001 A characteristic-type formulation of the

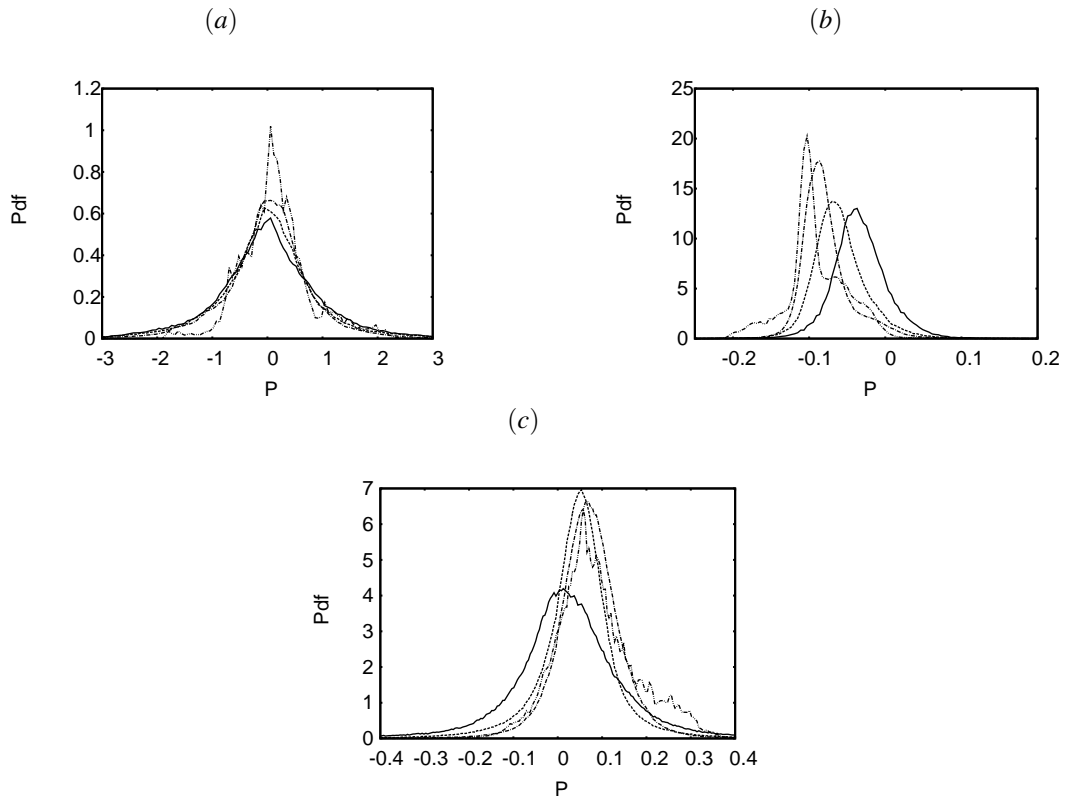


Figure 1: PDF of negative dilation (P) in (a) pipe, (b) nozzle, (c) diffuser. — viscous sublayer, - - - buffer layer, -.-.- log layer, -.-.- core region

Navier-Stokes equations for high order upwind schemes. *Computers and Fluids* **30**, 37–67.

Soria, J., Sondergaard, R., Cantwell, B.J., Chong, M.S. & Perry, A.E. 1994 A study of fine-scale motions of incompressible time-developing mixing layers. *Physics of Fluids* **6**, 871–884.

Suman, S. & Girimaji, S. 2010 Velocity gradient invariants and local flow-field topology in compressible turbulence.

Journal of Turbulence **11**.

Wang, Li & Lu, Xi-Yun 2012 Flow topology in compressible turbulent boundary layer. *Journal of Fluid Mechanics* **703**, 255–278.

Williamson, J. K. 1980 Low-storage Runge-Kutta schemes. *Journal of Computational Physics* **35**, 48–56.

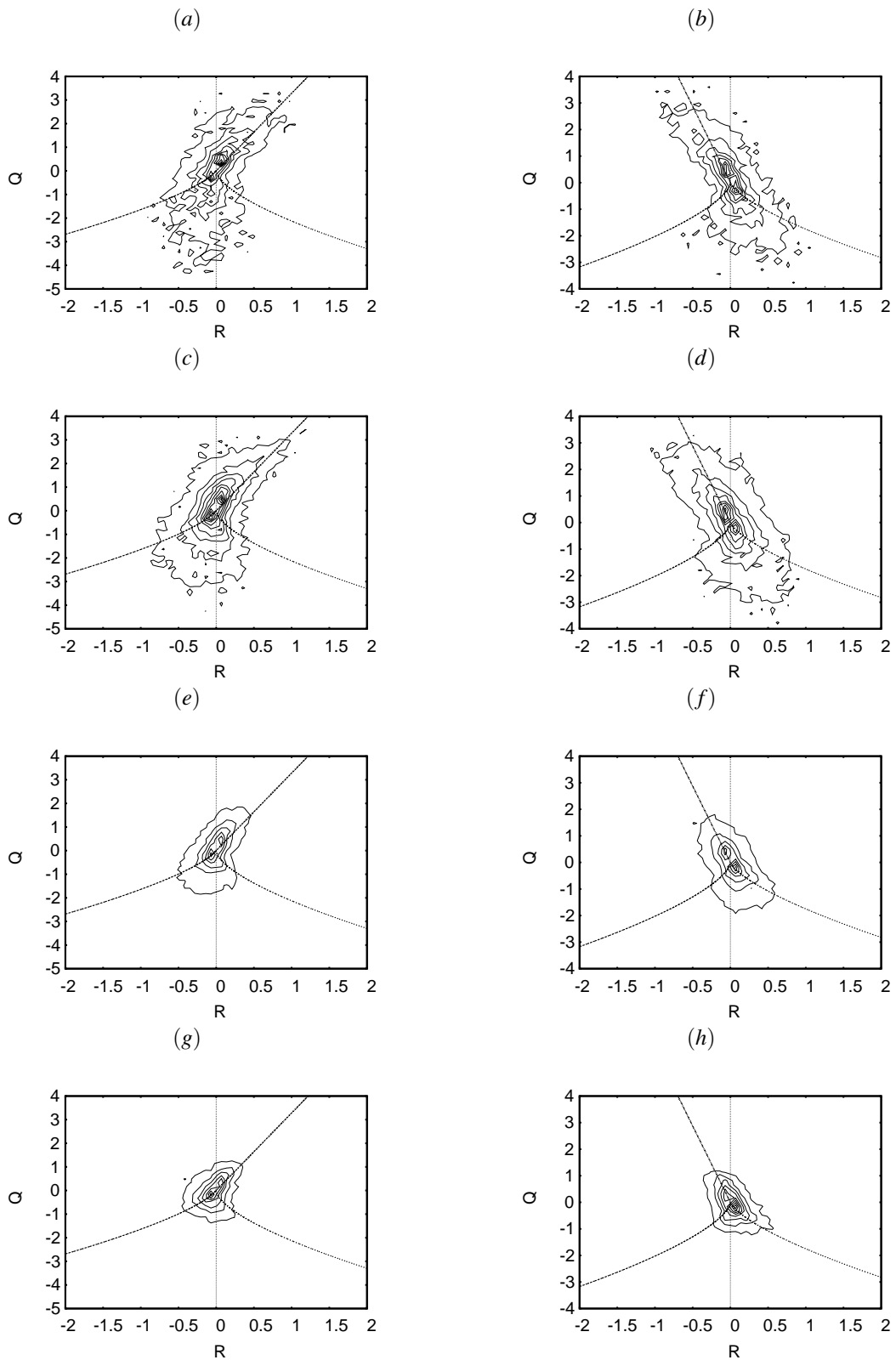


Figure 2: Isolines of joint pdf of Q and R for supersonic pipe flow for negative dilatation ($P = 0.3$) (a,c,e,g) and positive dilatation ($P = -0.174$) (b,d,f,h). a,b: viscous sublayer; c,d: buffer layer; e,f: log layer; g,h: core region

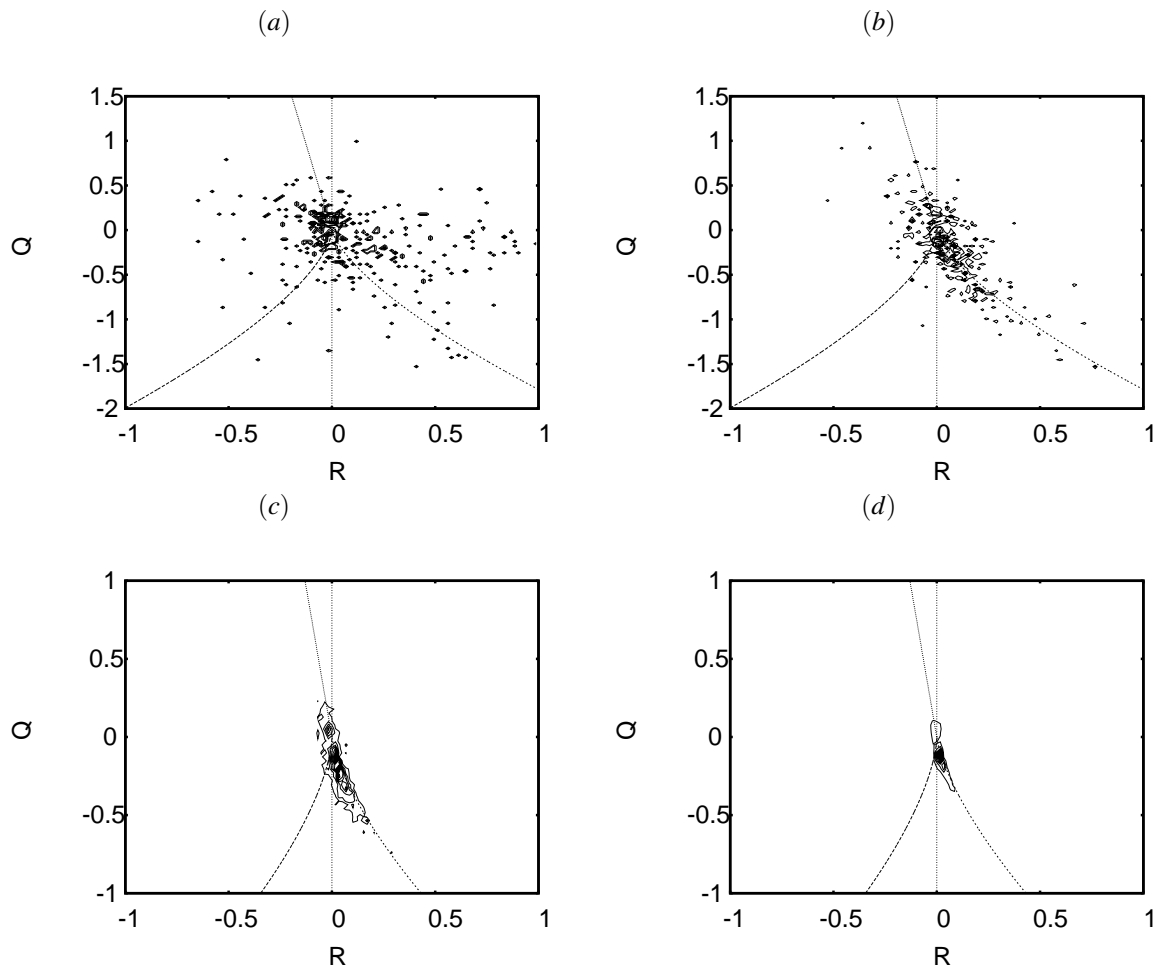


Figure 3: Isolines of joint pdf of Q and R for supersonic nozzle flow for positive dilatation ($P = -0.13$). a: viscous sublayer; b: buffer layer; c: log layer; d: core region

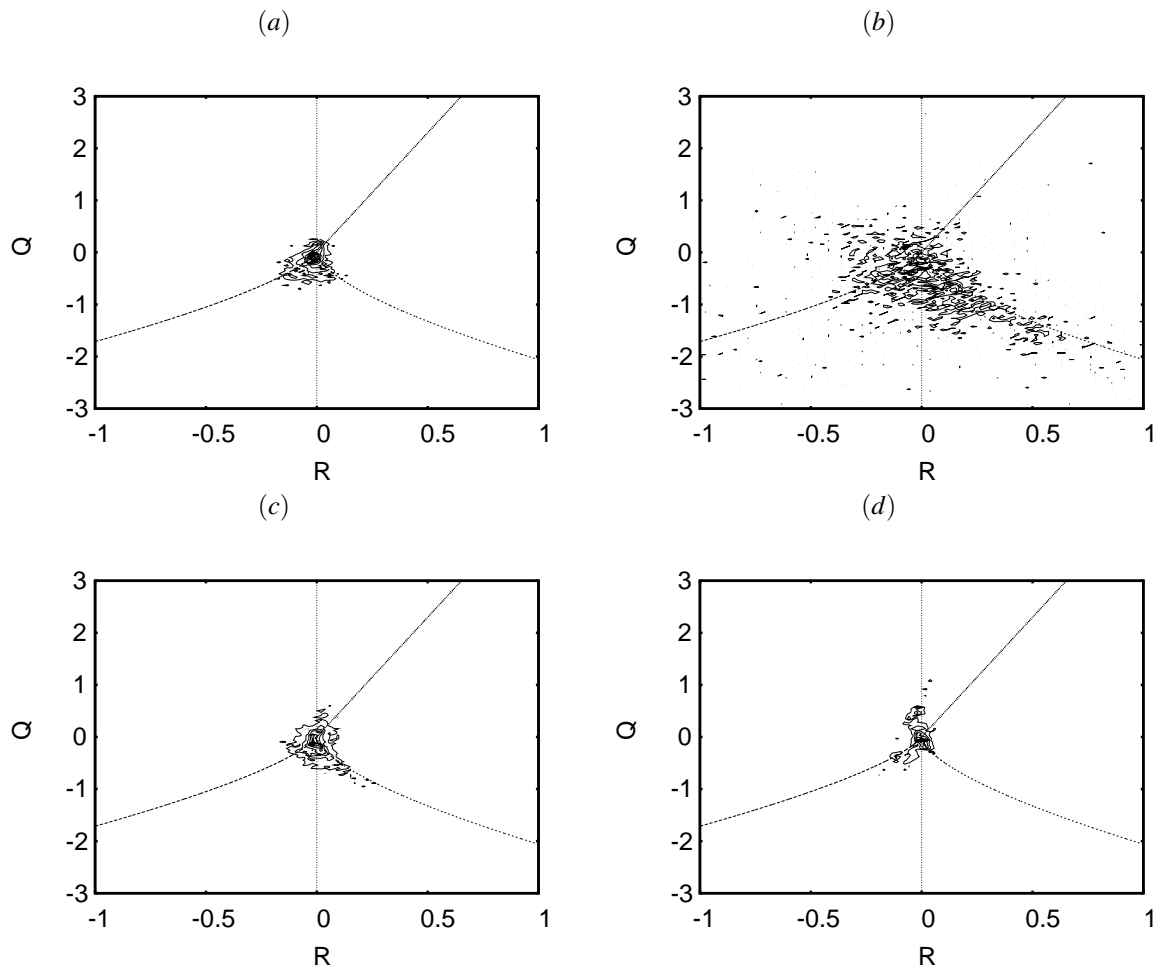


Figure 4: Isolines of joint pdf of Q and R for supersonic diffuser flow for negative dilatation ($P = 0.2175$). a: viscous sublayer; b: buffer layer; c: log layer; d: core region